IEEE Access
Multidisciplinary | Rapid Review | Open Access Journal

Received December 11, 2019, accepted January 12, 2020, date of publication January 15, 2020, date of current version January 24, 2020.

Digital Object Identifier 10.1109/ACCESS.2020.2966767

Optimal Trajectory Planning for 2-DOF Adaptive Transformable Wheel

KIJUNG KIM[1], YOUNGSOO KIM[1], JONGWON KIM[1], HWA SOO KIM[2], (Member, IEEE), AND TAEWON SEO[3], (Member, IEEE)

[1]School of Mechanical and Aerospace Engineering, Seoul National University, Seoul 08826, South Korea
[2]Department of Mechanical System Engineering, Kyonggi University, Suwon 16227, South Korea
[3]School of Mechanical Engineering, Hanyang University, Seoul 04763, South Korea

Corresponding authors: Hwa Soo Kim (hskim94@kgu.ac.kr) and Taewon Seo (taewonseo@hanyang.ac.kr)

This work was supported by the National Research Foundation of Korea under Grant NRF-2019R1A2C1008163 and Grant NRF-2016R1D1A1B03935516.

ABSTRACT Steps are frequently encountered while mobile robots move in indoor environments; thus, the ability to overcome a step is essential to indoor mobile robots. In this study, a new adaptive transformable wheel is conceptually proposed to effectively overcome steps of different sizes. The center trajectory of the proposed wheel is optimally designed to minimize its fluctuations while the robot overcomes a step. For this purpose, a kinematic analysis of the proposed wheel is performed to identify the points that its center must pass while the robot overcomes a step. The center trajectory is optimized with an objective function to evaluate the mobile stability of the proposed wheel under kinematic constraints to avoid undesired interferences between the wheel and the step. Extensive simulations with different steps verify that the optimal trajectory ensures stable and effective overcoming of steps. The experiment using the prototype of mobile robot equipped with the proposed wheel verifies the smoothness of resulting trajectory of wheel center.

INDEX TERMS Mobile robot, step, transformable wheel, trajectory planning.

I. INTRODUCTION

As the demand for various indoor applications such as guidance, cleaning, delivery, and health care, etc., has increased, mobile robots for indoor applications have received considerable attention [1]–[7]. It is noted that most of these robots move via the wheel mechanism owing to the simplicity of the structure and the high efficiency on a flat surface. Unfortunately, the wheel mechanism has the inherent defects for overcoming structured obstacles such as steps and stairs, which are frequently encountered in indoor environments. For the wheel to overcome a step passively, the diameter of the wheel must be two times larger than the height of the step [8]. Furthermore, because wheeled mobile robots may suffer from unexpected fluctuations and impacts while overcoming steps or stairs, for safe operation, their speed becomes significantly lower than that on flat ground [2], [5].

Many investigations have been performed to resolve such limitations of wheeled mobile robots, which can be classified into two categories. In the first category, passive links are incorporated with the wheel mechanism. For example, the Rocker–Bogie mechanism has been widely adopted to enhance the obstacle-overcoming ability of wheeled mobile robots such as the Shrimp Rover and the CRAB, etc [2], [8]–[11]. However, because most of these mobile robots were developed to overcome obstacles on rough terrain, they are not suitable for indoor applications. Even though active links such as tracks have been attached to the wheel mechanism [4], [12], a vertical riser for steps or stairs is indispensable for wheeled mobile robots to overcome these obstacles. Recently, an additional passive link (called a ''Tusk'') was used to create an angle of attack for the initial and climbing steps so that the mobile robot with the Tusk can climb stairs without a riser; however, the angle of the Tusk must be adjusted according to the size of the stairs [13]. Modification of the Tusk with tracks or active links has also been proposed to overcome various stairs with large nose or without risers [14].

The second category involves changing the wheels of mobile robots from circular to another shape. For example, the Wheel Transformer can quickly overcome a step whose

The associate editor coordinating the review of this manuscript and approving it for publication was Hui Xie.

height is 3.5 times larger than the wheel radius through the tactful design of the two-degrees of freedom (DOF) transformable wheel, but it still requires a riser to overcome steps since the transformation of the wheel is triggered by the friction between the wheel and the riser [15]. The Quattroped can overcome steps without a riser by using two-DOF half-circle wheels; however, it must completely stop twice for the wheel alignment during overcoming steps [16]. It is noted that both the Wheel Transformer and the Quattroped can overcome higher steps or stairs than circular wheeled robots but cannot overcome steps or stairs without a vertical riser at a high moving speed. It is noted that the transformed wheel shape and size of the Wheel Transformer and the Quattroped are uniquely determined; thus, the size of the steps or stairs that they can overcome is restricted. Additionally, the resulting motions for overcoming a step or stair have not been fully analyzed, even though they are important for judging the mobile stability.

To resolve these limitations effectively, a new adaptive transformable wheel consisting of three lobes is proposed herein. The size and shape of this wheel can be changed by adjusting the radius of the wheel and the tilting angle of each lobe at the same time so that the proposed wheel allows a mobile robot to overcome various sizes of steps and stairs continuously and quickly in comparison with the existing transformable wheel-based mobile robots. The main goal of this study is to ensure the ability of the mobile robot to stably overcome various steps and stairs via the proposed adaptive transformable wheel. In this study, we focused on overcoming a step because stair-overcoming is identical to the continuous repetition of step-overcoming.

First, the whole procedure of overcoming a step was analyzed in order to kinematically determine how to change the wheel shape along each axis and when to transform its shape along the center trajectory of the proposed wheel. Additionally, a performance index (PI) was introduced to evaluate the motion of the proposed wheel while overcoming steps from the viewpoint of mobile stability. Then, the optimal center trajectory of the proposed wheel was designed to minimize this index. The main focus of previous investigations on transformable wheels [15], [16] and the passive link with tracks [14] was to overcome obstacles without considering the center trajectory of the wheel. However, in this study, the center trajectory of the proposed wheel was optimally designed by combining continuous transformation of the wheel to ensure that the mobile robot could stably overcome obstacles like steps and stairs. The extensive simulations were conducted with various steps to prove the viability of optimal trajectory planning for the proposed wheel.

The remainder of this paper is organized as follows. In Section II, the new adaptive transformable wheel is introduced, along with its design parameters. A kinematic analysis of the proposed wheel is performed to derive constraints on its trajectory during overcoming a step. In Section III, the PI for evaluating the step-overcoming ability of the proposed wheel is defined, and under constraints, the optimal trajectory planning for the proposed wheel is done. The optimal trajectory obtained in Section III is compared with the general trajectory obtained without the optimization in Section IV by using the PI. With the prototype of 2-DOF wheel, the experimental result is briefly introduced. Finally, concluding remarks are presented in Section V.

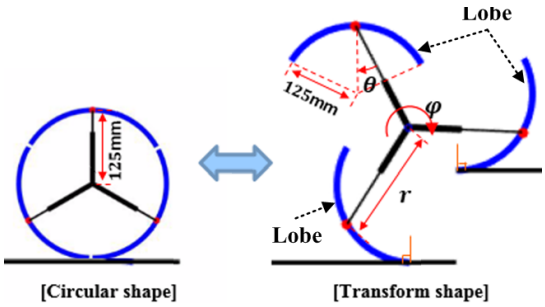

FIGURE 1. Concept of the adaptive transformable wheel.

II. NEW TRANSFORMABLE WHEEL

A. CONCEPT OF ADAPTIVE TRANSFORMABLE WHEEL

The adaptive transformable wheel is proposed in this study to overcome steps effectively. As shown in Fig. 1, the proposed adaptive transformable wheel has two DOFs: along the r-direction and the θ-direction. Through the transformation, the radius of the proposed wheel can change from 125 mm (in the circular shape) to 220 mm (in the transformed shape), and the tilting angle of each lobe is within the range of $\pm$ 40°. The lobe of the proposed wheel can rotate in both the clockwise and counter-clockwise directions; thus, a mobile robot equipped with the proposed wheel can change its direction of movement on the spot without additional steering or rotating. Unlike wheels of the Wheel Transformer and the Quattroped, the proposed adaptive transformable wheel is characterized by its continuous transformability against obstacles of different sizes. By choosing the proper variations of the radius and tilting angle, the center trajectory of the proposed wheel can be sufficiently smoothed to ensure that the mobile robot stably overcomes steps.

Fig. 2 presents examples of the required transformation of the proposed wheel for climbing stairs of different sizes without any interference, where the horizontal and vertical axes correspond to the lengths of the tread and riser, respectively. As shown in Fig. 2, the sizes of the treads and risers of the stairs range from 260 mm to 340 mm and from 100 mm to 180 mm, respectively. The sizes (tread $\times$ riser) of the stairs denoted as (s1), (s2), (s3), and (s4) are 260 mm $\times$ 180 mm, 340 mm $\times$ 180 mm, 260 mm $\times$ 100 mm, and 340 mm $\times$ 100, respectively. While stairs (s1) and (s3) have the same riser lengths, stairs (s2) and (s4) have the same tread lengths. Fig. 2 shows that as the slope of the stair becomes steeper, i.e., closer to (s1), the tilting angle of the lobe increases. Additionally, as the tread of the stair becomes larger, i.e., closer to (s4), the radius of the proposed wheel increases. It is noted that as the length of the tread increases, the distance between the end point of the lobe contacting the ground and

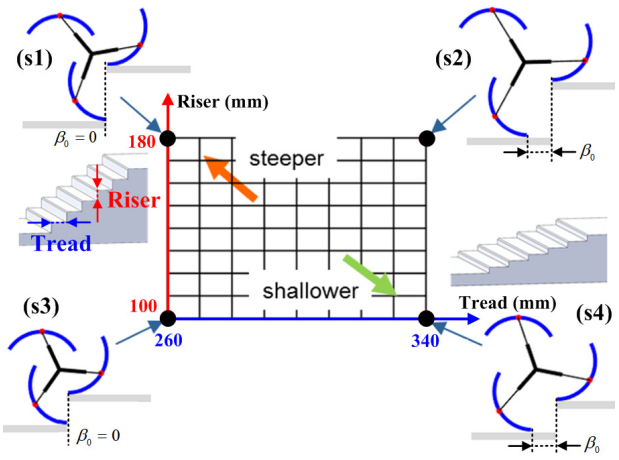

FIGURE 2. Examples of the required transformation of the proposed adaptive transformable wheel with stairs of different sizes.

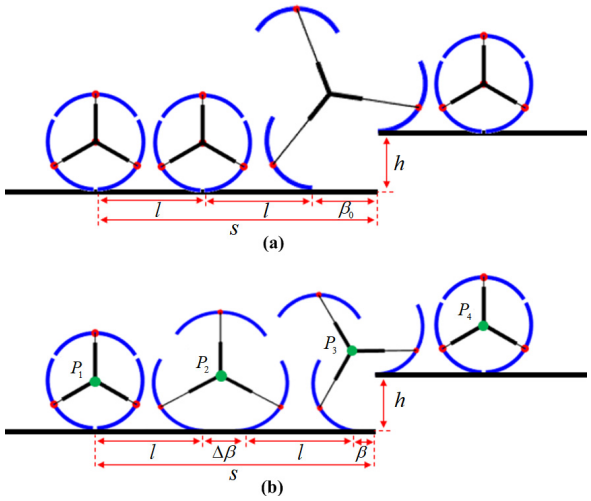

FIGURE 3. Cases of step-overcoming with transformation of the proposed wheel.

the riser of the stair (denoted as β_0) increases regardless of the length of the riser, as shown in Fig. 2.

B. KINEMATIC ANALYSIS OF STEP-OVERCOMING

Two cases of step-overcoming with transformations of the proposed wheel are shown in Fig. 3, where l, h, and s represent the circumference of the lobe, the height of the obstacle, and the initial distance between the wheel and the step, respectively. Recall that β_0 corresponds to the distance between the end point of the lobe contacting the ground and the step when the proposed wheel cannot move forward in the circular shape, owing to the possibility of collision. Thus, β_0 is obviously smaller than l, and the distance s can be expressed by $s = n \times l + \beta_0$, as shown in Fig. 3, where $n = 2$. The proposed wheel shown in Fig. 3(a) continuously rotates in the circular shape until encountering a step, but the proposed wheel shown in Fig. 3(b) starts to transform its shape slightly before encountering a step, which can reduce β_0 by introducing the additional movement $\Delta\beta$, as shown in Fig. 3(b). Consequently, the initial distance s can be divided into the detailed regions, i.e., $s = 2l + \beta + \Delta\beta$, and the required radius of the transformed wheel in Fig. 3(b) is significantly smaller than that of the transformed wheel in Fig. 3(a).

Thus, the resulting height of the center of the proposed wheel is reduced while the robot overcomes the step. In Fig. 3(b), the center of the proposed wheel to pass mandatorily is denoted as P_i, with $i = 1, 2, 3, 4$. The points P_1 and P_4 are determined by the initial and final positions of the wheel, respectively, however the points P_2 and P_3 are determined by $\Delta\beta$ and β, respectively. Because the required radius of the proposed wheel increases in proportion to β_0, it is necessary to reduce β_0 by using the linear transform to slightly adjust the radius of the proposed wheel without changing its tilting angle while passing the point P_2, as shown in Fig. 3(b).

III. OPTIMAL TRAJECTORY PLANNING

A. OBJECTIVE FUNCTION

The indoor mobile robot usually has a small width but a high center of mass similar to an inverted pendulum; thus, even small fluctuations may be detrimental to its stability. Therefore, it is important to reduce the effect of the impact on the robot body when the robot overcomes a step. Notably, such undesired fluctuation mainly occurs when the robot changes its lobes contacting the ground. In particular, owing to the drastic change of the contact surfaces, the mobile robot climbing a step is prone to undergo a large fluctuation and at this moment, the acceleration of the wheel center is increased significantly [3]. Therefore, it is important to minimize the maximum acceleration of the wheel center to reduce the undesired effect of such a large fluctuation. If the wheel center fluctuates frequently, the direction of its speed changes often; consequently, the energy consumption may be increased since a center trajectory is enlarged. From this viewpoint, to reduce the frequent fluctuation of the wheel center, the average acceleration of the wheel center must be minimized during overcoming a step.

Accordingly, a PI for the proposed wheel to overcome a step is defined to minimize the maximum and average accelerations simultaneously, as follows:

$$\mathrm{PI} = \min \left\{ \max\left(|\vec{a}|\right) + \frac{\sum |\vec{a}|}{n} \right\} \tag{1}$$

where n represents the total number of points chosen in the trajectory. The constraint on the center trajectory is combined with the PI in Eq. (1) to mitigate the effect of unexpected jerk on the robot body, which can be ensured by the C2 continuity of the center trajectory [17]. Other constraints related to the kinematics of the proposed wheel are examined in detail in the following section.

B. PATH GENERATION

The first step for trajectory planning for the proposed wheel is to generate a path for the wheel center, i.e., select the function f_i (with $i = 1, 2, 3$) as the path for the proposed wheel, which can connect the points P_i (with $i = 1, 2, 3, 4$).

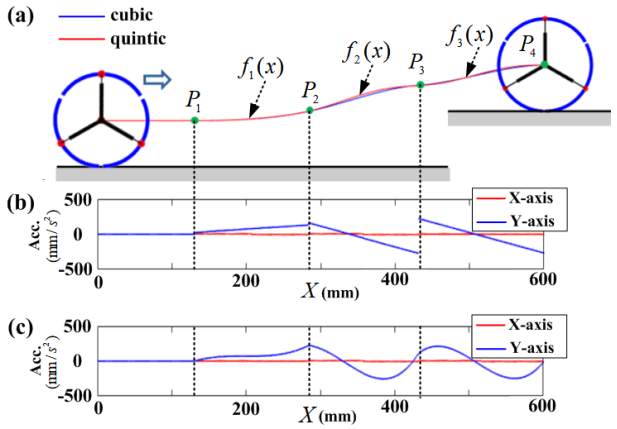

FIGURE 4. Cases of step-overcoming with transformation of the proposed wheel.

Since the proposed wheel passes the points P_1 and P_4 in the circular shape, the corresponding slopes and curvatures at these points are assumed to be zero without loss of generality. Although the points P_2 and P_3 can be uniquely determined by $\Delta\beta$ and β, the corresponding slopes and curvatures at these points are still unknown. Therefore, after choosing the proper slopes (a_2,a_3) and curvatures (c_2,c_3) at the points P_2 and P_3 with β, the polynomial $f_i(x) = \sum_{k=0}^{m} b_{i,k}\, x^k$ (with $i = 1, 2, 3$) can be obtained by solving Eqs. (2) and (3):

$$f(P_{i,x}) = P_{i,y} \tag{2}$$

$$f'(P_{i,x}) = \begin{cases} a_i & (i = 2,\ 3) \\ 0 & (i = 1,\ 4) \end{cases},$$

$$f''(P_{i,x}) = \begin{cases} c_i & (i = 2,\ 3) \\ 0 & (i = 1,\ 4) \end{cases} \tag{3}$$

where $P_{i,x}$ and $P_{i,y}$ represent the x- and y-components of the point P_i, respectively, and the slope and curvature at the point P_i are expressed by a_i and c_i, respectively.

Fig. 4 presents examples of trajectory planning with cubic ($m = 3$) and quintic ($m = 5$) polynomials. As shown in Fig. 4(a), the center trajectories obtained from the cubic and quintic polynomials are similar. However, as shown in Figs. 4(b) and 4(c), the trends of the resulting accelerations exhibit large discrepancies: while all the accelerations along the Y-axis obtained by both the cubic and quintic polynomials are continuous, the acceleration along the Y-axis obtained by the cubic polynomial is discontinuous at the points P_2 and P_3, and the acceleration along the Y-axis obtained by the quintic polynomial is continuous and significantly smoother than that obtained by the cubic one. This is because the minimum order of the polynomial for satisfying the conditions of the position, slope, and curvature of the curve simultaneously is 5. Thus, in this study, the quintic polynomial is chosen for f_i, with $i = 1, 2, 3$.

C. TRAJECTORY PLANNING

Trajectory planning is done to determine the movement of the wheel center with the aim of ensuring the continuity of its corresponding acceleration on the given path in Section 3.2.

It is worthwhile to note that the mass of the wheel and its distribution are not considered in the trajectory planning. Instead, it is assumed that the wheel keeps in contact with the ground without slip so that only the rolling occurs while the wheel moves on the ground with a sufficiently large contact friction and driving force, which seems acceptable because the maximum required friction coefficient for the proposed wheel is expected quite smaller than existing mechanisms due to its unique ability to transform its shape [18]. Also, the length of the lobe and the radius of the wheel are set to be 260 mm and 125 mm, respectively. Now, the j^{th} position of the center trajectory is denoted as (x_j^c, y_j^c), satisfying $y_j^c = f_i(x_j^c)$. The moving distances of the proposed wheel along the X- and Y-axes are divided by the steps $\Delta x_j^c = x_j^c - x_{j-1}^c$ and $\Delta y_j^c = y_j^c - y_{j-1}^c$ with the time interval Δt. Then, the corresponding accelerations a_x^c and a_y^c along the X- and Y-axes and the curvature $c_{y/x}$ are represented as follows:

$$a_x^c = \frac{x_{j+1}^c - 2x_j^c + x_{j-1}^c}{\Delta t^2} = \frac{\Delta x_{j+1}^c - \Delta x_j^c}{\Delta t^2} \tag{4}$$

$$a_y^c = \frac{y_{j+1}^c - 2y_j^c + y_{j-1}^c}{\Delta t^2} = \frac{\Delta y_{j+1}^c - \Delta y_j^c}{\Delta t^2} \tag{5}$$

$$c_{y/x} = \frac{y_{j+1}^c - 2y_j^c + y_{j-1}^c}{(\Delta x_j^c)^2} = \frac{\Delta y_{j+1}^c - \Delta y_j^c}{(\Delta x_j^c)^2} \tag{6}$$

If the step along the X-axis is constant, i.e., $\Delta x_{j+1}^c = \Delta x_j^c = \Delta_x$, the resulting acceleration a_x^c along the X-axis is zero and continuous according to Eq. (4). Because the path f_i (with $i = 1, 2, 3$) generated in Section 3.2 satisfies the condition of C2 continuity, the curvature $c_{y/x}$ obtained from f_i is continuous, and consequently, the continuity of the acceleration a_y^c is guaranteed by Eqs. (5) and (6). Therefore, with the constant step along the X-axis for the time interval Δt, the center trajectory can be built to ensure the continuity of acceleration along both the X- and Y-axes.

The proposed wheel has three DOFs: two DOFs along the r-direction and the θ-direction for wheel transformation and one DOF along the φ-direction for wheel rotation. Because only two DOFs are necessary to determine the wheel center, the remaining DOF must be determined in a different way. The point of the lobe contacting the ground is determined by the rotation of this lobe, which implies that the reaming DOF is determined by the contact point of the lobe. As shown in Fig. 5(a), the position of the wheel center and the contact point of the lobe completely determine the current position and shape of the proposed wheel. It is assumed that similar to the constant movement of the wheel center, the contact point of the lobe moves with a constant step size Δ_p, which can reduce the required variations of the proposed wheel along both the r- and θ-directions. In summary, for the path in Section 3.2, the trajectory of the wheel center for ensuring the continuity of acceleration and the trajectory of the contact point for reducing the required variation of the proposed wheel are chosen, which gives the full information of r, θ, and φ to determine the position and shape of the proposed wheel for overcoming a step.

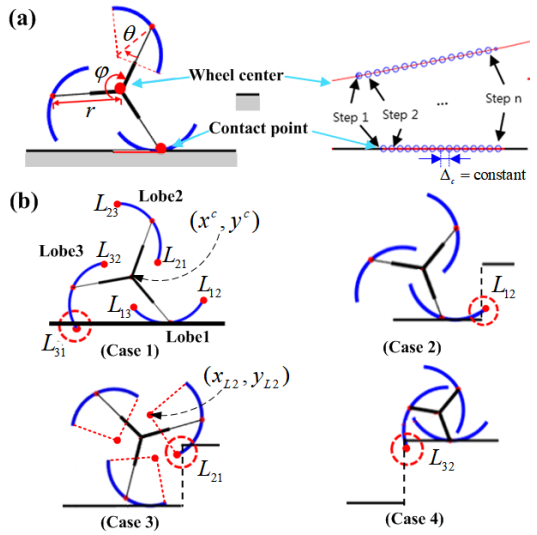

FIGURE 5. (a) Geometric relationship between the wheel center and the contact point and (b) kinematic constraints for overcoming a step.

D. KINEMATIC CONSTRAINTS

In computing the movement of the proposed wheel with the wheel center and the contact point of the lobe, it is necessary to investigate when the interference between the proposed wheel and a step occurs, which must be reflected in the movement of the proposed wheel to prevent failure in overcoming the step.

Fig. 5(b) presents four cases of interferences between the proposed wheel and a step. As shown, the interferences mainly occur between the end points of all lobes and the step. The x- and y-components of the end point of lobe i adjacent to lobe j are denoted as $(L_{ij})_x$ and $(L_{ij})_y$, respectively, as shown in Fig. 5(b), and the wheel center is denoted as (x^c,y^c). In case 1, the end point L_{31} of lobe 3 interferes with the ground along the Y-axis when the proposed wheel starts to transform its shape, which is expressed as follows:

$$(L_{31})_y = y^c - r\sin(\tfrac{5\pi}{6}+\varphi) + 125\cos(\varphi+\theta) < 0 \qquad (7)$$

In cases 2–4, all the lobes of the proposed wheel may have interference with the step while the robot overcomes the step. The interference between lobe 1 of the proposed wheel and the step may occur when β becomes smaller than 0, because lobe 1 is too close to the step. The interference between lobe 2 and the riser of the step may occur when the y-component of lobe 2 is smaller than the height of the step and the distance between the center (x_{L2},y_{L2}) of lobe 2 and the edge of the step is smaller than the radius r_2 of lobe 2, as shown in Fig. 5(b):

$$\begin{cases} (L_{21})_y = x^c + r\cos\varphi - 125\sin(\dfrac{5\pi}{6} - \varphi - \theta) < h \\ \sqrt{(x_{L2}-s)^2 + (y_{L2}-h)^2} < r_2 \end{cases} \qquad (8)$$

where

$$\begin{cases} x_{L2} = x^c + r\sin\varphi - 125\sin(\varphi+\theta) \\ y_{L2} = y^c + r\cos\varphi - 125\cos(\varphi+\theta) \end{cases} \qquad (9)$$

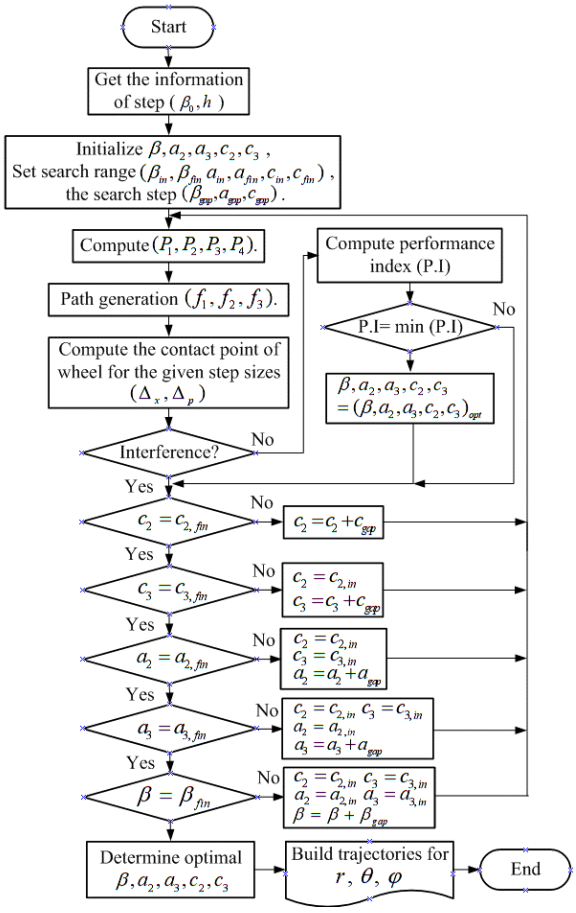

FIGURE 6. Flowchart for optimal trajectory planning.

Finally, lobe 3 may have interference with the riser of the step when the wheel changes its shape from the transformed one to the circular one after overcoming the step, as shown in Fig. 5(b). This is expressed as follows:

$$\begin{cases} (L_{32})_x = x^c - r\cos(\dfrac{5\pi}{6}+\varphi) + 125\sin(\varphi+\theta) > s \\ (L_{32})_y = y^c - r\sin(\dfrac{5\pi}{6}+\varphi) + 125\cos(\varphi+\theta) < h \end{cases} \qquad (10)$$

IV. OPTIMIZATION AND DISCUSSION

A. OPTIMIZATION

The design parameters β, a_2, a_3, c_3, and c_2 are optimized using MATLAB. A detailed flowchart of the optimal trajectory planning is shown in Fig. 6.

In summary, the information of the step, such as the distance from the contacting lobe of the proposed wheel to the riser of the step and the height of the step, is first given. Then, the search range $(\beta_{in}, \beta_{fin}, a_{in}, a_{fin}, c_{in}, c_{fin})$ and the search step $(\beta_{gap}, a_{gap}, c_{gap})$ are selected for each parameter. With the initial value of β, the point P_i $(i = 1,\cdots, 4)$ is computed. Thus, the path f_i passing the point P_i can be constructed with initial values of a_2, a_3, c_2, and c_3. For the generated path f_i, the wheel center $(x^c,\ y^c)$ and the corresponding contact point of the lobe are computed with constant step sizes Δ_x

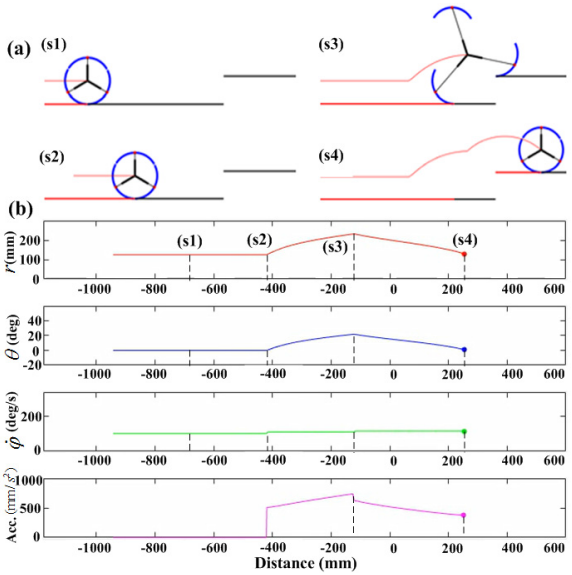

FIGURE 7. Simulation results without optimization: (a) trajectory of wheel center and (b) corresponding radius, tilting angle, angular speed of rotating angle of proposed wheel and acceleration of wheel center.

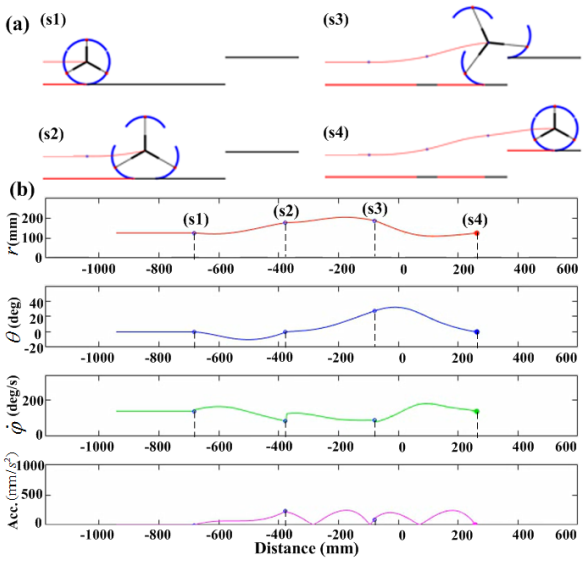

FIGURE 8. Simulation results with optimization: (a) trajectory of wheel center and (b) corresponding radius, tilting angle, angular speed of rotating angle of proposed wheel and acceleration of wheel center.

and Δ_p, respectively. From the computed wheel center and contact point, the shape of the proposed wheel is uniquely determined, and it is ascertained whether the current shape and location of the proposed wheel interfere with the step or not. If interference with the step occurs, each parameter is sequentially tuned within a search step, as shown in Fig. 6, and the point P_i $(i = 1, \cdots, 4)$ is recomputed. Otherwise, the corresponding PI is checked to determine whether it is minimized or not. For the entire ranges of the parameters β, a_2, a_3, c_3, and c_2, the optimization procedure is repeated to identify the optimal parameter set $(\beta, a_2, a_3, c_2, c_3)_{opt}$. Additionally, for various steps with different starting points and heights (s,h), the optimization procedure is conducted in a similar manner.

B. SIMULATIONS AND EXPERIMENT

For fair comparison, a simulation to overcome a step without the optimization was performed, where the total simulation time was equal to that required for the simulation with the optimization but the transformation to add the movement $\Delta\beta$ was not done. In the simulation without the optimization, the radius and tilting angle r and θ were assumed to change linearly in proportion to each other during the step-overcoming.

In Fig. 7, the simulation results without the optimization for overcoming a step 150 mm in height are shown, where the circumference of the lobe was 260 mm and the distance from the starting point to transform the shape of the wheel to the riser of the step was 234 mm ($\beta_0 = 0.9l$). As shown in Fig. 7, the step had no vertical wall between two horizontal planes, indicating that any wheel that employs the friction from the vertical wall for climbing cannot climb up this type of step. In Fig. 7(a), the trajectory of the wheel center is shown, along with a detailed description of each stage. The proposed wheel started to change its shape at stage **(s2)** and to climb up the step at stage **(s3)**; that is, lobe 2 of the proposed wheel began to contact the upper side of the step. Fig. 7(b) shows the corresponding radius and tilting angle r and θ, the angular speed of the rotating angle $\dot{\varphi}$ and the acceleration of the wheel center, respectively. While the angular speed of the rotating angle $\dot{\varphi}$ was kept relatively constant, the radius and tilting angle of the proposed wheel changed significantly in the short time duration. At the stage **(s2)**, the acceleration was likely to undergo a drastic change from 0 to 500 mm/s^2. Moreover, this higher acceleration was maintained during the remaining stages.

Fig. 8 shows the results of the simulation with the optimized trajectory. The step height and the size of wheel were same as those used in the previous simulation. The proposed wheel changed its radius in order to generate the additional movement before climbing the step so that when the wheel starts to climb the step, the location of stage **(s2)** is moved further to the right, as shown in Fig. 8(a) and the resulting distance between the wheel and the vertical riser of step becomes much closer than that of **(s3)** shown in Fig. 7(a). The effect of this linear transformation is readily observed in Fig. 8(a), where the radius of the proposed wheel of **(s3)** in Fig. 8(a) is smaller than that **(s3)** in Fig. 7(a) so that the resulting trajectory is smoother than the previous one in Fig. 7(a) and especially, in comparison with the trajectory of the wheel center in Fig. 7(a), the trajectory of the wheel center in Fig. 8(a) is significantly smoother at stages **(s2)** and **(s3)**; thus, the motion of robot for overcoming the step did not suffer from fluctuations.

Additionally, it is noteworthy that the acceleration of wheel center in Fig. 8(b), obtained by the optimization is kept below a certain level for the entire time duration even with some changes. Furthermore, the acceleration of wheel center in Fig. 8(b) is considerably smaller than that in Fig. 7(b),

TABLE 1. Optimization results for various condition on the initial distance and the height of the step.

h	150 mm			180 mm		
β_0	$0.3l$	$0.6l$	$0.9l$	$0.3l$	$0.6l$	$0.9l$
β	0.20	0.26	0.47	0.21	0.25	0.46
a_2	10	13	13	13	13	13
a_3	-1	4	7	-2	3	6
c_2	0.002	0.002	0.001	0.006	0.0025	0.0015
c_3	0.0005	0.001	0	0.002	0	-0.001
PI	910 (28%)	383 (69%)	200 (82%)	1152 (23%)	523 (63%)	332 (76%)

which implies that when moving the proposed wheel with the optimized trajectory, less driving force may be required to lift the mobile robot for overcoming a step and as a result, the energy consumption could be enhanced (please, refer to the supplementary video files for detailed information regarding the simulation).

Table 1 shows the simulation results with the optimization for various conditions on the initial distance and the height of the step, where the percentage corresponds to the ratio of reduction of PI through the optimization. The results confirm that as the step height increased and the initial distance from the proposed wheel to the step decreased, the PI was likely to be degraded, possibly because as the slope of the obstacle increased, the slope of the trajectory of the wheel center and the required acceleration were inevitably increased in order to complete the entire transformation of the proposed wheel for the given short distance β_0. Also, as the distance β_0 decreased, the possibility of interference between the proposed wheel and the step significantly increased; thus, it was difficult to satisfy the constraints, and consequently, the ratio of reduction of PI by the optimal trajectory planning decreased as shown in Table 1. Therefore, it is important to allow a sufficient distance to the proposed wheel, which can adjust the distance between it and the step optimally by the linear transformation.

Fig. 9 shows the detailed mechanical design of a 2-DOF adaptive transformable wheel. As shown in Figs. 9(b) and 9(c), the lobe of proposed wheel can rotate in the counter-clockwise (CCW) and clockwise (CW) directions by operating the upper- and lower-side motors (denoted by red color), respectively. Also, by operating both the upper- and lower-side motors simultaneously, the radius of proposed wheel can be increased or decreased as in Fig. 9(d). It is noteworthy that the proposed wheel in Fig. 9 can separate the wheel rotation from the wheel transformation by tactfully combing belts with DC motors. In Fig. 10, the experimental results using the prototype of mobile robot equipped with the proposed wheels are shown, where the height of real step is about 170 mm. Even though the mobile robot is supported by the additional links for stable climbing, the center trajectory of wheel in Fig. 10 is quite smooth and comparable to that of track-wheel mechanism [3], [4]. It is noted that the

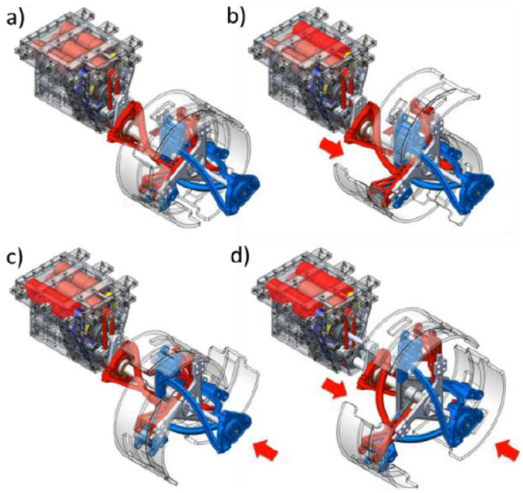

FIGURE 9. (a) Mechanical design of 2-DOF adaptive transformable wheel, (b) rotation of lobe in CCW direction, (c) rotation of lobe in CW direction and (d) change of wheel radius.

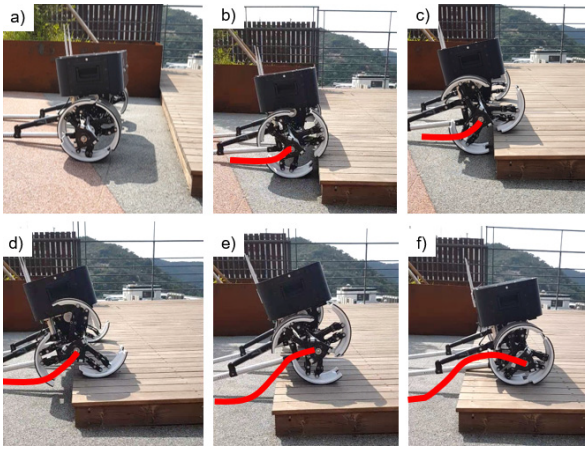

FIGURE 10. Experimental result by using the prototype of mobile robot equipped with the proposed wheel controlled by the proposed algorithm.

step in Fig. 10 has a nose, which may be a big hurdle to general wheel-based mechanisms. As confirmed in Fig. 10, the prototype of mobile robot enables to climb the step stably with the help of the proposed transformable wheel.

V. CONCLUSION

This study presents an optimal trajectory planning method for improving the stability of a mobile robot equipped with a new adaptive transformable wheel to overcome a step. Through a kinematic analysis of the proposed wheel, the entire trajectory of the wheel for overcoming a step was examined, five design parameters to guarantee the smooth motion of the wheel were selected, and a PI was defined to evaluate the mobile stability of the optimized trajectory. For two steps of 150 and 180 mm in the height and different initial distances, the optimization of the trajectory planning was performed using MATLAB. The optimization reduced the PI by 82% maximally, and the resulting trajectory of the wheel center became much smoother significantly; thus, little fluctuation was observed, and any detrimental effect

of impact caused by the fluctuations on the mobile robot could be reduced. Through the simulations with a decreasing distance β_0, it is observed that the optimal values of β, a_2, and a_3 were determined to prevent interferences while c_2 and c_3 were selected to satisfy the C2 continuity of the path.

In the near future, we are going to improve the step-climbing ability of 2-DOF adaptive transformable wheel-based robot by virtue of advanced control methodology based on a precise dynamic model for the proposed wheel in order to ensure fast and stable locomotion on flat surfaces and various sizes of steps and stairs. We hope that after enhancing the mechanical design of the prototype in Fig. 9, the detailed analysis and experimental verifications are going to be shared in the next publication.

REFERENCES

[1] M. Eich, F. Grimminger, and F. Kirchner, "A versatile stair-climbing robot for search and rescue application," in *Proc. IEEE Int. Workshop Saf., Secur. Rescue Robot.*, Oct. 2008, pp. 35–40.

[2] D. Kim, H. Hong, H. S. Kim, and J. Kim, "Optimal design and kinetic analysis of a stair-climbing mobile robot with rocker-bogie mechanism," *Mech. Mach. Theory*, vol. 50, pp. 90–108, Apr. 2012.

[3] D. Choi, Y. Kim, S. Jung, H. S. Kim, and J. Kim, "Improvement of step-climbing capability of a new mobile robot RHyMo via kineto-static analysis," *Mech. Mach. Theory*, vol. 114, pp. 20–37, Aug. 2017.

[4] D. Choi, Y. Kim, S. Jung, J. Kim, and H. S. Kim, "A new mobile platform (RHyMo) for smooth movement on rugged terrain," *IEEE/ASME Trans. Mechatronics*, vol. 21, no. 3, pp. 1303–1314, Jun. 2016.

[5] H. Hong, D. Kim, H. S. Kim, S. Lee, and J. Kim, "Contact angle estimation and composite locomotive strategy of a stair-climbing mobile platform," *Robot. Comput.-Integr. Manuf.*, vol. 29, no. 5, pp. 367–381, Oct. 2013.

[6] M. Tarokh and G. Mcdermott, "Kinematics modeling and analyses of articulated rovers," *IEEE Trans. Robot.*, vol. 21, no. 4, pp. 539–553, Aug. 2005.

[7] J. Choi, K. Jeong, and T. Seo, "Pol-E: Large-obstacle overcoming based on energy conversion method using an elastic link," *Int. J. Control Autom. Syst.*, vol. 15, no. 4, pp. 1835–1843, Aug. 2017.

[8] R. Siegwart, P. Lamon, T. Estier, M. Lauria, and R. Piguet, "Innovative design for wheeled locomotion in rough terrain," *Robot. Auto. Syst.*, vol. 40, nos. 2–3, pp. 151–162, Aug. 2002.

[9] M. D. Berkemeier, E. Poulson, and T. Groethe, "Elementary mechanical analysis of obstacle crossing for wheeled vehicles," in *Proc. IEEE Conf. Robot. Autom. (ICRA)*, May 2008, pp. 2319–2324.

[10] T. Thueer, P. Lamon, A. Krebs, and R. Siegwart, "CRAB-exploration rover with advance obstacle negotiation capabilities," in *Proc. 9th ESA Workshop Adv. Space Technol. Robot. Automat.*, Nov. 2006.

[11] C.-K. Woo, H. D. Choi, S. Yoon, S. H. Kim, and Y. K. Kwak, "Optimal design of a new wheeled mobile robot based on a kinetic analysis of the stair climbing states," *J. Intell. Robot. Syst.*, vol. 49, no. 4, pp. 325–354, Jul. 2007.

[12] S. Jung, D. Choi, H. S. Kim, and J. Kim, "Trajectory generation algorithm for smooth movement of a hybrid-type robot Rocker–Pillar," *J. Mech. Sci. Technol.*, vol. 30, no. 11, pp. 5217–5224, Nov. 2016.

[13] J. Choe, M. C. Hah, H. Kim, and U. Kwon, "TuskBot: Design of the mobile stair climbing 2 by 2 wheels robot platform with novel passive structure tusk," in *Proc. 3rd Int. Conf. Control, Autom. Robot. (ICCAR)*, 2017, pp. 217–220.

[14] J. Choi, U. Kwon, M. C. Hah, and H. Kim, "Design analysis of TuskBot: Universal stair climbing 4-wheel indoor robot," in *Proc. IEEE Conf. Intell. Robots Syst. (IROS)*, Sep. 2017, pp. 6908–6914.

[15] Y.-S. Kim, G.-P. Jung, H. Kim, K.-J. Cho, and C.-N. Chu, "Wheel transformer: A wheel-leg hybrid robot with passive transformable wheels," *IEEE Trans. Robot.*, vol. 30, no. 6, pp. 1487–1498, Dec. 2014.

[16] S.-C. Chen, K.-J. Huang, W.-H. Chen, S.-Y. Shen, C.-H. Li, and P.-C. Lin, "Quattroped: A leg–wheel transformable robot," *IEEE/ASME Trans. Mechatronics*, vol. 19, no. 2, pp. 730–742, Apr. 2014.

[17] S. Macfarlane and E. Croft, "Jerk-bounded manipulator trajectory planning: Design for real-time applications," *IEEE Trans. Robot. Autom.*, vol. 19, no. 1, pp. 42–52, Feb. 2003.

[18] Y. Kim, J. Kim, H. S. Kim, and T. Seo, "Curved-spoke tri-wheel mechanism for fast stair-climbing," *IEEE Access*, vol. 7, pp. 173766–173773, 2019.

KIJUNG KIM received the B.S. degree in mechanical engineering from Sungkyunkwan University, South Korea, in 2016, and the M.S. degree in mechanical engineering from Seoul National University, South Korea, in 2018. His research interest includes the areas of mobile robot designs.

YOUNGSOO KIM received the B.S. and Ph.D. degrees in mechanical engineering from the School of Mechanical and Aerospace Engineering, Seoul National University, South Korea, in 2013 and 2019, respectively. His research interest includes the areas of robot mechanism design.

JONGWON KIM received the B.S. degree in mechanical engineering from Seoul National University, South Korea, in 1978, the M.S. degree in mechanical and aerospace engineering from the Korea Advanced Institute of Science and Technology (KAIST), South Korea, in 1980, and the Ph.D. degree in mechanical engineering from the University of Wisconsin–Madison, USA, in 1987. He is currently a Professor with the School of Mechanical and Aerospace Engineering, Seoul National University. His current research interests include parallel mechanisms, Taguchi methodology, and field robots.

HWA SOO KIM (Member, IEEE) received the B.S. and Ph.D. degrees in mechanical engineering from Seoul National University, South Korea, in 2000 and 2006, respectively. From 2007 to 2008, he was a Postdoctoral Researcher with the Laboratory for Innovations in Sensing, Estimation and Control, University of Minnesota, MN, USA. He is currently an Associate Professor with the Department of Mechanical System Engineering, Kyonggi University. His current research interests include design, modeling, and control of various mobile platforms, such as wall-cleaning robot and stair-climbing robot.

TAEWON SEO (Member, IEEE) received the B.S. and Ph.D. degrees from the School of Mechanical and Aerospace Engineering, Seoul National University, South Korea. He was a Postdoctoral Researcher with the Nanorobotics Laboratory, Carnegie Mellon University, a Visiting Professor with the Biomimetic Millisystems Laboratory, UC Berkeley, and an Assistant Professor with the School of Mechanical Engineering, Yeungnam University, South Korea. He is currently an Associate Professor with the School of Mechanical Engineering, Hanyang University, South Korea. His research interests include robot design, analysis, control, optimization, and planning. He received the Best Paper Award of the IEEE/ASME TRANSACTIONSON MECHATRONICS, in 2014. He is also a Technical Editor of the IEEE/ASME TRANSACTIONSON MECHATRONICS and an Associate Editor of the IEEE ROBOTICSAND AUTOMATION LETTERS and *Intelligent Service Robots*.